OPEN

SQUARE GRID DEFORMATION ANALYSIS OF THE MACULA AND POSTOPERATIVE METAMORPHOPSIA AFTER MACULAR HOLE SURGERY

SUN HO PARK, MD,*† KEUN HEUNG PARK, MD,*† HWA YEONG KIM, MD,*† JAE JUNG LEE, MD,*† HAN JO KWON, MD,*‡ SUNG WHO PARK, MD, PHD,*† IK SOO BYON, MD, PHD,*‡ JI EUN LEE, MD, PHD*†

Purpose: To investigate the correlation between postoperative metamorphopsia and macular deformation after macular hole surgery.

Methods: This study included 28 eyes of 28 patients who underwent vitrectomy and internal limiting membrane removal for an idiopathic macular hole. The retinal vasculatures were compared between preoperative and postoperative photographs, and postoperative deformation of the macula was assessed as deformation of the square grid. The displacement of each node was measured, and deformation of the grid was calculated as differences in the coordinates of the adjacent nodes. These parameters were analyzed to find correlation with metamorphopsia measured using the M-charts after 6 postoperative months.

Results: The average deformations in the vertical and horizontal lines of the grid were 94.29 μm and 49.72 μm, respectively. Perifoveal deformation was significantly greater than parafoveal deformation (P = 0.001$\sim$0.019). The multiple regression analysis demonstrated that the vertical M-score correlated with superior perifoveal deformation of the vertical line on the fovea (P = 0.036), and the horizontal M-score correlated with temporal perifoveal deformation of the horizontal line on the fovea (P = 0.032).

Conclusion: The parafoveal tissue was displaced with the fovea concurrently after internal limiting membrane removal in macular hole surgery causing perifoveal deformation, which correlated with postoperative metamorphopsia.

RETINA 41:931–939, 2021

The anatomic success rate of macular hole (MH) surgery and visual outcomes have improved with the advancements in surgical procedures, including various manipulation techniques for the internal limiting membrane (ILM).[1–4] Although closure of MH can be achieved in almost all patients using the recent techniques, functional outcomes, such as the visual field defect, scotoma, and metamorphopsia, are not satisfactory.[5–7] In particular, postoperative metamorphopsia is a major complaint after successful MH closure.

Several studies have reported displacement of the fovea to the optic disk after ILM removal.[8–10] A detailed analysis demonstrated that the retina in the macular region was displaced centripetally, nasally, and slightly inferiorly.[11,12] The temporal macula was more displaced compared with the nasal macula.[10–12] The degree of displacement correlated with the extent of ILM removal.[11] Interestingly, observations of foveal asymmetric elongation seem conflicting with the other reports.[13,14] Asymmetric elongation in the nasal part of the fovea was correlated with postoperative metamorphopsia especially in the group with a small extent of ILM peel rather than that with a large-extent peel.

However, no previous reports provided plausible explanations for the different patterns of macular deformation based on the extent of ILM removal. Furthermore, despite the general agreement that macular deformation is associated with postoperative metamorphopsia after ILM removal, the exact mechanisms are debated.

The purpose of this study was to investigate the mechanisms of postoperative metamorphopsia after

MH surgery with ILM removal by correlating grid deformation of the macula directly with metamorphopsia measured using M-charts.

Methods

This study was a retrospective, interventional, consecutive case series. The study protocol was approved by the Institutional Review Board of Pusan National University Hospital (1905-026-079) and complied with the tenets of the Declaration of Helsinki.

The consecutive patients with an idiopathic MH who achieved MH closure after undergoing pars plana vitrectomy with ILM removal in the period from 2015 to 2018 were included in the study. All patients were operated by a single surgeon (J.E.L.). Phacoemulsification was combined concurrently with the phakic eyes. The ILM was removed to an extent of approximately 3 disk diameters (DDs). The vitreous cavity was filled using the filtered air in all eyes at end of the operation.

The exclusion criteria were apparent epiretinal membrane, high myopia more than −5 D, a fundus image of poor quality, and other retinal diseases that may cause biases in the interpretation of retinal displacement. Patients who underwent vitrectomy with an inverted ILM flap procedure and no ILM removal were also excluded.

Sets of fundus photographs acquired at the baseline and after 6 postoperative months, using the same fundus camera, were collected. Similar to a previous report, we included a set of 2 photographs in which the disk overlapped with a disparity less than 0.5 DD, to minimize the biases caused by the peripheral image distortion.[11]

From the *Department of Ophthalmology, School of Medicine, Pusan National University, Yangsan, South Korea; †Biomedical Research Institute, Pusan National University Hospital, Busan, South Korea; and ‡Research Institute of Convergence of Biomedical Science and Technology, Pusan National University Yangsan Hospital, Yangsan, South Korea.

J. E. Lee: Bayer (consultant, honoraria, travel grant, and research fund), Novartis (consultant, honoraria, and research fund), Allergan (consultant and honoraria), Alcon (honoraria), AbbVie (consultant and honoraria), Samsung Biopeis (consultant). The remaining authors have no financial/conflicting interests to disclose.

Reprint requests: Ji Eun Lee, MD, PhD, Department of Ophthalmology, School of Medicine, Pusan National University Hospital, 179, Gudeok-ro, Seo-gu, Busan 49241, South Korea; e-mail: jlee@pusan.ac.kr

Metamorphopsia was measured using M-charts (Inami Co, Tokyo, Japan) after 6 postoperative months. First, the vertical lines were used, and subsequently, the horizontal lines were used after rotating the M-charts by an angle of 90°. The examinations were performed three times, and the average value was recorded.[15]

The extent of ILM removal was measured in an en face optical coherence tomography (OCT) image at ILM segmentation[16] and converted to the optic DD unit (1 DD = 1.8 mm).[17]

Macular deformation was analyzed as the deformed grid using the custom software (Figure 1). The 6 × 6-mm square grid having crossing lines at an interval of 1 mm was overlaid on the preoperative photograph. The grid size was determined corresponding to the visual angle of the M-chart lines because a visual angle of 1° was projected on the macula with 288-μm length (20° × 0.288 mm = 5.76 mm).[18] The grid was located by placing the center node at the center of the MH base in the preoperative en face OCT image. Each node was anchored at the preoperative photograph, which was deformed by moving the node to match the retinal vasculature with that of the postoperative photograph (Figure 1). The postoperative location of the foveal center was defined by reviewing the serial OCT B-scans to find the ellipsoid zone signal changes and marked in the postoperative en face OCT image, as previously reported.[16] The center node was moved to the marked position after matching the retinal vasculature of the postoperative photograph and that of the en face image.

The horizontal and vertical displacements of each node were measured. Deformations of the vertical and horizontal lines were calculated as the absolute differences in the x-coordinate and y-coordinate between the adjacent nodes, respectively. Parafoveal deformation was defined as the difference in coordinates between the center node and the first adjacent node, and perifoveal deformation was defined as the difference between the first and second nodes. The line segment was labeled after the area of the horizontal or vertical line. Figure 2 demonstrates the indexed nodes and segment lines.

Statistical Analysis

The Snellen acuity was converted to the corresponding logarithm of minimum angle of resolution. The values are expressed as mean ± SD. The Wilcoxon signed-rank test was performed to analyze the displacement of the node. The Mann–Whitney *U* test was used to compare the deformation between the parafoveal and perifoveal areas. The Spearman

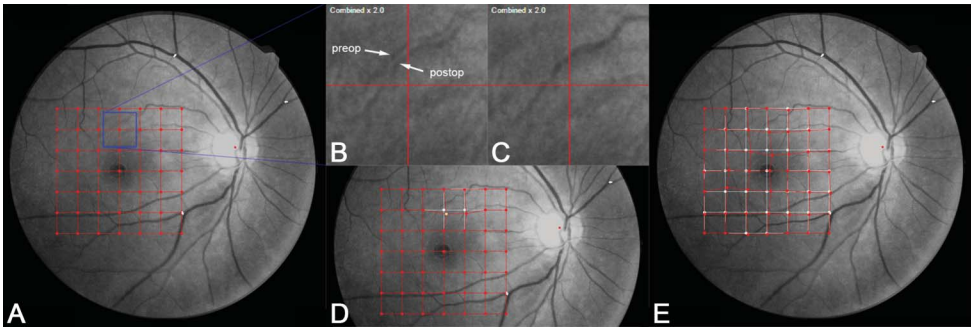

Fig. 1. A. Preoperative and postoperative fundus photographs of patients with an MH have been overlapped in the custom software. The major retinal vessels are matched between two photographs by registering three bifurcating points on each photograph. The 6 × 6-mm grid having crossing lines at 1-mm interval is superimposed on the photograph. **B.** In the magnifying window, both of the preoperative and postoperative retinal vessels are seen indicating the macula was deformed after surgery. **C.** Moving the node of the grid deforms the preoperative photograph, and the retinal vasculatures of two photographs are matched. **D.** The deformation of the macula is assessed in two nodes. **E.** Measurements are completed in all 49 nodes.

correlation coefficient test determined the significance of associations between the M-score and the various parameters. A multiple regression analysis was conducted to find the independent parameters. All statistical analyses were performed using the SPSS software for Windows, version 22.0 (SPSS, Inc, Chicago, IL). P value <0.05 was considered statistically significant.

Results

We included 28 eyes of 28 patients (17 men and 11 women) who met the eligibility criteria. The mean minimum MH diameter was 416.1 ± 147.4 μm, and the extent of ILM removal was 3.41 ± 0.46 DD. The visual acuity improved from 0.72 ± 0.24 (equivalent to Snellen 20/105) to 0.28 ± 0.15 logarithm of minimum angle of resolution (20/38) after 6 postoperative months. The vertical and horizontal M-scores were 0.35 (0.0–1.5) and 0.25 (0.0–1.0) in median (range).

Table 1 shows the average displacements of the nodes, and Figure 3 presents them schematically. To describe the deformation in general, the parafoveal area was deformed centripetally and displaced to the optic disk while maintaining the rectangular configuration. Consequently, the perifoveal deformation was most distinct.

The average displacements of all nodes were 34.90 μm nasally in the x-coordinate and 11.97 μm inferiorly in the y-coordinate. The average displacements of the central nine nodes were 97.83 μm toward the optic disk and 13.81 μm downward.

The average deformations were 94.29 μm on the vertical lines and 49.72 μm on the horizontal lines. Table 2 presents the deformations of the parafoveal and perifoveal segments. Significant differences were noted between the parafoveal and perifoveal deformation in HCT and HCN segments of the horizontal line (P = 0.001 and 0.017) and in VCL, VCU, and VTL segments of the vertical lines (P = 0.001, 0.019, and 0.049, respectively).

The M-score showed a significant correlation with several displacements and deformation values. The horizontal M-score had a significant correlation with vertical displacement at three nodes in the foveal center and temporal area (r = 0.385–0.424,

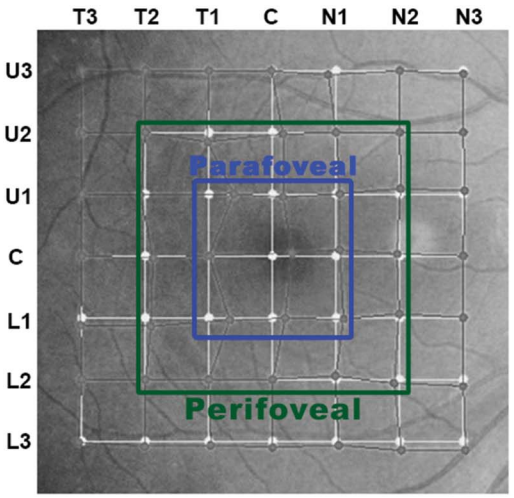

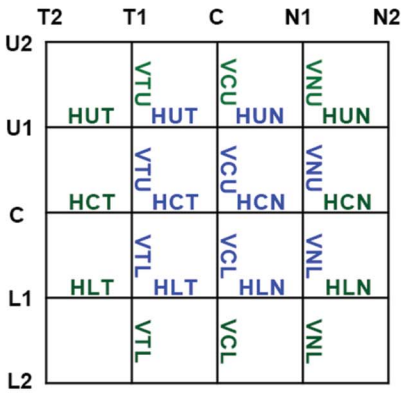

Fig. 2. Definition of the parafoveal, perifoveal, horizontal, and vertical segments to correlate their deformation with the M-score. The abbreviations represent the topographic locations as follows: H, horizontal; V, vertical; C, central; U, upper; L, lower; N, nasal; T, temporal. The blue and green letters indicate the parafoveal and perifoveal segments, respectively.

Table 1. The Average Displacement of Each Node After Macular Hole Closure (Mean ± SD)

Displacement (μm)		T3	T2	T1	Cx	N1	N2	N3
U3	X	−11.50 ± 59.46	−2.83 ± 67.64	−0.34 ± 45.92	+8.13 ± 79.78	+18.38 ± 59.99	+5.45 ± 25.16	−12.86 ± 50.93
	Y	+0.97 ± 45.71	+1.88 ± 42.44	+12.07 ± 45.30	+16.20 ± 58.71	+5.74 ± 58.01	−19.65 ± 51.65	−12.62 ± 52.40
U2	X	−22.53 ± 73.33	+9.10 ± 77.55	+69.11 ± 52.04*	+84.33 ± 81.70*	+29.66 ± 44.97*	+12.53 ± 40.99	+5.65 ± 27.47
	Y	0.84 ± 56.80	20.06 ± 56.11†	35.23 ± 61.53*	+66.74 ± 61.47*	+60.09 ± 60.38*	+32.18 ± 71.89†	+6.29 ± 55.91
U1	X	+2.62 ± 66.92	+47.00 ± 78.07*	+157.76 ± 123.93*	+167.44 ± 96.31*	+53.05 ± 82.41*	+17.54 ± 42.09†	+1.40 ± 29.17
	Y	9.31 ± 28.02†	+13.00 ± 32.67	+32.47 ± 55.79†	+66.94 ± 62.33*	+48.43 ± 72.79*	+14.36 ± 43.65	−3.57 ± 41.97
Cy	X	+9.53 ± 76.82	+78.45 ± 113.00*	+103.85 ± 100.40*	+121.21 ± 69.44*	+8.24 ± 61.96	+33.47 ± 69.77†	+12.64 ± 39.89
	Y	+3.49 ± 22.80	+12.07 ± 59.27	+18.39 ± 20.83	+1.23 ± 20.97	+14.47 ± 52.61	−3.70 ± 62.94	+7.71 ± 38.66
L1	X	−26.50 ± 63.54†	+31.63 ± 86.48†	+143.79 ± 104.44*	+158.85 ± 105.12*	+49.70 ± 66.31*	+27.75 ± 65.48†	−0.10 ± 32.04
	Y	+27.18 ± 51.24*	+26.71 ± 70.21†	+0.93 ± 60.99	−21.29 ± 77.98	−36.50 ± 79.33†	+0.75 ± 65.76	+19.38 ± 52.93
L2	X	−21.66 ± 70.23	−0.35 ± 78.86	+38.73 ± 58.74*	+41.19 ± 67.35*	+19.81 ± 42.15†	+15.29 ± 54.38	+1.71 ± 36.12
	Y	+10.53 ± 46.50	+35.10 ± 73.64†	+2.50 ± 62.38	+15.04 ± 82.02	−0.13 ± 82.22	+5.06 ± 56.80	+12.61 ± 42.78
L3	X	−10.62 ± 59.97	−15.39 ± 62.31	−15.29 ± 68.76	+10.65 ± 43.81	−1.27 ± 24.89	−7.50 ± 20.14	+1.92 ± 19.59
	Y	+17.04 ± 51.51	+18.36 ± 59.96	+33.22 ± 68.27†	+22.99 ± 66.76	+29.36 ± 76.85†	+21.64 ± 47.63†	+17.73 ± 52.33

A positive value represents displacement of the node toward the optic disk on the x-coordinate and upward displacement on the y-coordinate. T, temporal; C, central; N, nasal; U, upper; L,lower; X, horizontal; Y; vertical. Refer to Figure 2 for the locations of each node.

*Significant at $P < 0.01$.

†Significant at $P < 0.05$.

P = 0.024–0.043) and with deformation at the perifoveal temporal segment of the horizontal line on the fovea (perifoveal HCT segment, r = 0.472, P = 0.011). The vertical M-score was correlated with the horizontal displacement of three nodes in the perifoveal area (r = 0.40–0.513, P = 0.005–0.032) and with deformation at the perifoveal upper segment of the vertical line on the fovea (perifoveal VCU segment, r = 0.384, P = 0.044).

The multiple regression analysis revealed that deformation on the horizontal line of the perifoveal HCT segment (P = 0.032, β = 0.406) and vertical displacement of the nodes in the foveal center (P = 0.018, β = 0.425) were significantly associated with the horizontal M-score. The vertical M-score was only correlated with the deformation of the perifoveal VCU segment on the vertical line (P = 0.036, β = 0.654, Figures 3 and 4).

Discussion

The parafoveal tissue was displaced concurrently after pars plana vitrectomy with ILM peeling, and postoperative metamorphopsia correlated with the perifoveal deformation. These results would provide the explanations for the controversies arising from previous studies.

As mentioned in the introduction section, the findings from previous reports seemed incoherent and conflicting. However, we reviewed them meticulously and found a pattern based on the extent of ILM peeling—small extent versus large extent. For example, large-extent peeling resulted in foveal displacement to the optic disk with slight expansion in the size of the foveal avascular zone[12] or foveal pit.[14,16] The temporal retinal vessels were more displaced compared with the nasal.[11,12] By contrast, after small-extent peeling, the foveal pit expanded with significant asymmetric elongation to the nasal and superior sides. In addition, whole macular displacement was associated with the extent of ILM peeling,[11] but foveal asymmetry was significantly greater in a small-extent group and was associated with postoperative metamorphopsia.[14]

In earlier reports, fundus photographs and cross-sectional OCT images were used to measure macular deformation after MH surgery. Some studies evaluated the displacement by measuring the changes in distance between certain points on the macula.[9,10,19] In our previous study,[11] vascular displacement was assessed using the grid comprising 16 sectors in 2 rings. However, these previous methods had the disadvantage of not being able to analyze the direct association between M-score and macular deformation. Compared

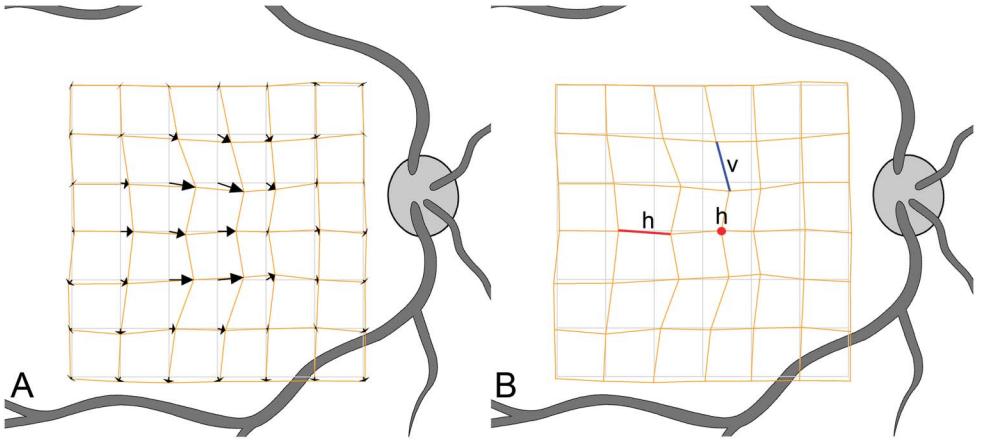

Fig. 3. Macular deformation, assessed in the displacement of the retinal vasculature after surgical closure of MH, is presented as the square grid deformation. **A.** The arrow represents the average displacement in each node. The displacement of each node is enlarged three times that of the actual displacement for enhancing visualization. **B.** The color coding indicate a significant correlation with the M-score in the multiple regression analysis. The blue color represents a significant correlation with the vertical M-score (v) and the red with the horizontal M-score (h).

with previous methods, the strength of this study was that we could quantitatively evaluate the deformation of not only the foveal center but the entire macula in detail by measuring the displacement at 49 nodes on the square grid. Moreover, quantifying deformation of the horizontal and vertical lines enabled direct correlation with the horizontal and vertical M-scores, respectively.

The patients complained of metamorphopsia both before and after the MH operation. Preoperative metamorphopsia was commonly manifested as pincushion distortion in the Amsler grid and was proposed to have arisen from an eccentric displacement of the photoreceptors.[20] Quantification of metamorphopsia using M-charts demonstrated that it improved significantly after MH closure without ILM peeling. Postoperative metamorphosia in the ILM-peeled eye is believed to consist of at least two components: residual and induced after ILM removal.

Several mechanisms have been suggested regarding the directions of the macular displacements in eyes after MH closure with ILM peeling. The recent articles suggested that postoperative macular deformation would result from the combination of several factors. The ILM is the basement membrane of the Müller cells, and its removal leads to loss of the structural support of the neural tissues of the retina. This enables the retina to be displaced because the ILM is a relatively nonelastic tissue preventing the deformation of the retina.[8,21,22] In addition, it was speculated that ILM peeling promotes the retinal nerve fiber (RNF) to shrink from where the ILM has been removed.[10] The RNF consists mainly of microtubules, and depolymerization of the microtubules may cause neuronal contractions.[23] As the optic nerve fibers are tethered to the lamina cribrosa, the macular tissues move toward the optic disk through contractions of the RNFs. Thus, the greater displacement of the temporal retina can be explained by proportional displacement of the tissues farther from the optic disk. Centripetal contractions through MH closure and gravity or buoyance were also suggested as compositions of the combined force.[9,11]

Table 2. Deformation on the Vertical and Horizontal Lines in the Parafoveal and Perifoveal Area After Surgical Closure of Macular Hole

Deformation on Horizontal Lines						
Segment	HUN	HUT	HCN*	HCT*	HLN	HLT
Parafoveal	59.33	59.39	37.30	18.92	36.44	57.01
Perifoveal	53.86	47.32	61.13	58.53	58.68	49.88
Deformation on Vertical Lines						
Segment	VNU	VNL	VCU*	VCL*	VTU	VTL*
Parafoveal	77.26	58.97	66.66	69.59	103.65	86.10
Perifoveal	67.70	54.31	99.65	124.41	101.11	116.87

*Significant differences between parafoveal and perifoveal area ($P < 0.05$).

C, central; H, horizontal; L, lower; N, nasal; T, temporal; U, upper; V, vertical.

However, these theories could not explain all the previous observations, especially asymmetric elongation of the foveal tissues after small-extent ILM peeling. The salient flaw was the assumption that the RNFs were tethered to the optic disk. In our previous study, superimposition of the preoperative and postoperative fundus photographs clearly demonstrated that the macular deformation occurred almost exclusively within the area from where the ILM was removed.[16] This observation suggested two important things. First, the contraction of the remnant ILM would play a limited role in macular deformation. Second, the tethered point should be the margin of the ILM removal, not the optic disk for the postoperative macular deformation through RNF contraction.

When the RNFs are tethered to the ILM, macular deformation by RNF contraction after ILM removal is

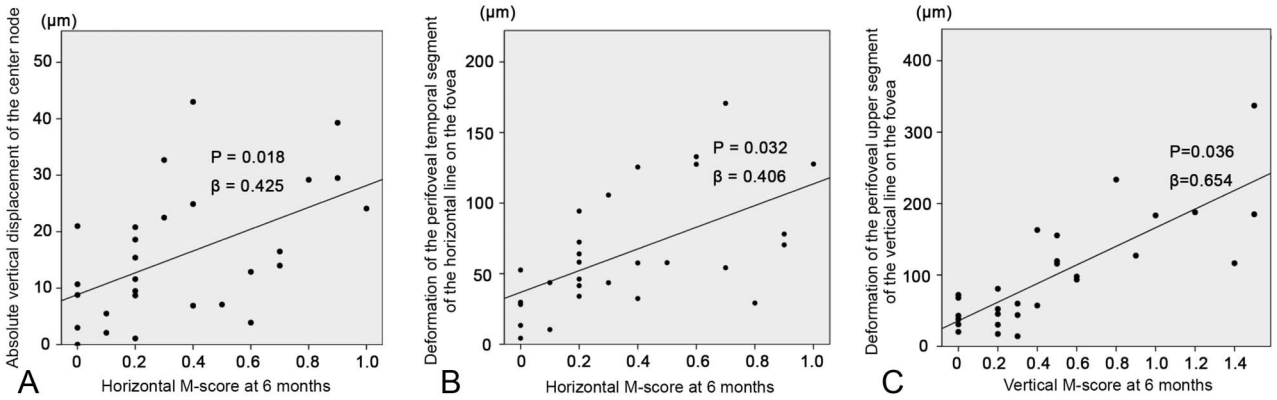

Fig. 4. Plot graphs showing the association between the M-score at 6 postoperative months and the factors that were significantly correlated in the multiple regression analysis. **A.** Vertical displacement of the center node had a significant correlation with the horizontal M-score (β = 0.425, *P* = 0.018). **B.** Deformation of the perifoveal temporal segment of the horizontal line on the fovea significantly correlated with the horizontal M-score (β = 0.406, *P* = 0.032). **C.** Deformation of the perifoveal upper segment of the vertical line on the fovea correlated with the vertical M-score (β = 0.654, *P* = 0.036).

expected as shown in Figure 5. In cases of small-extent ILM peeling of approximately 1.5 DD, the RNFs are arranged radially in the nasal half of the peeled area and are opposing vertically at the horizontal raphe in the temporal half (Figure 5A). The contraction forces would offset each other in the temporal area and expand the foveal depression in the nasal area. Accordingly, the foveal tissue would be elongated asymmetrically to the optic disk and, less remarkably, to the superior because of the arrangement of the RNFs (Figure 5B). These speculations are consistent with the observations by Bae et al.[14] In cases of large-extent ILM peeling of more than 3 DD, the RNFs from the horizontal raphe are exposed beyond the vertical midline on the foveal center, and the whole foveal tissue can be displaced with the RNF contraction forces (Figure 5C). Summation of all the vectors of RNF contraction and gravity would result in the foveal displacement to the optic disk and slightly inferiorly (Figure 5D). Our theory has no confliction with the observations of the previous articles, not only for large-extent peeling[8–12] but also for small-extent peeling.[14]

It is still unclear how deformation of the inner retina causes metamorphopsia in macular disorders. Several mechanisms have been suggested, including the optical fiber theory, synaptic disturbance theory, and photoreceptors disarrangement theory. According to the optical fiber theory, the retinal glial cells act as the optical fibers, which transmit incident light through the retinal surface to the photoreceptors.[24,25] When photons enter the Müller cells, which have been displaced from the original location, the photons finally reach the photoreceptors located away from the incident site. This irregular and wide stimulation of the photoreceptor cell layer may generate metamorphopsia. However, this theory cannot explain why a normal eye does not perceive monocular diplopia with pincushion distortion. As the Henle's fibers are arranged centrifugally from the outer to the inner retina, the Müller cells as optical fibers generate pincushion distortion and may result in monocular diplopia mixed with the image by the incident light straight through the sensory retina.

Hibi et al[26] found correlations between reduction in the thickness of the middle retinal layer and increase in the amplitude of the b-waves after epiretinal membrane peeling. This implicated that disturbances of the synaptic junctions may generate abnormal integration of signals from the photoreceptors, which may contribute in yielding sensations whose signals are not straightly aligned. Our results conflict this theory because the displacement of the parafoveal node was not significantly associated with postoperative metamorphopsia. If the synaptic aberration between the outer and the inner retina was the main mechanism of metamorphosia, it would correlate with the displacement of parafoveal nodes where the inner retina was displaced greater than the perifoveal area.

The photoreceptors disarrangement theory explains simply that metamorphopsia arises from an eccentric displacement of the photoreceptors due to an MH.[20] Our previous study demonstrated that the photoreceptor layer of the fovea was displaced with the inner retinal layer without disparity in the postoperative period after MH surgery with ILM removal and suggested that arrangement of the photoreceptors could be changed more readily than expected.[16] These findings

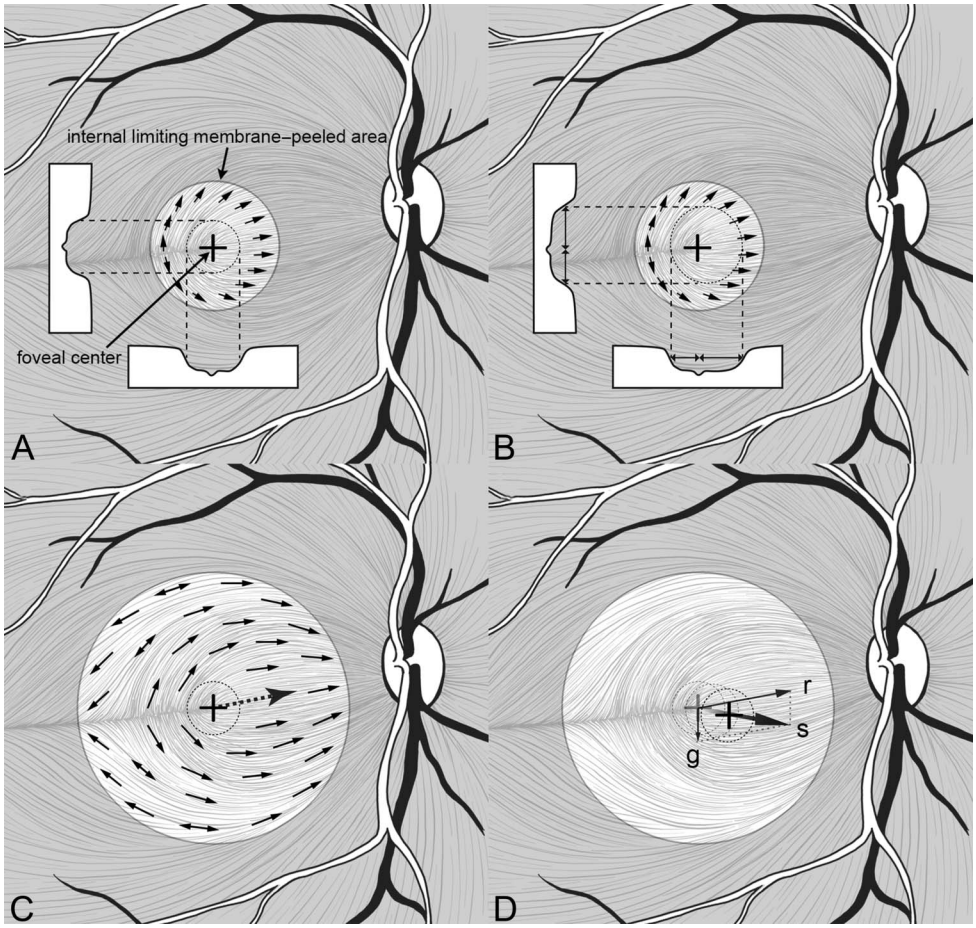

Fig. 5. Explanations for macular deformation due to RNF contraction after ILM removal. The dotted lines indicate the foveal depression, and the small arrows represent the deforming forces of the RNF contraction. **A.** When the ILM is removed to a small extent, the RNFs are arranged radially in the nasal half and are opposing vertically at the horizontal raphe in the temporal half of the peeled area. **B.** The contraction forces will offset each other in the temporal area and will expand the foveal depression in the nasal area, resulting in an asymmetric elongation of the foveal tissue. **C.** When the ILM is removed to a large extent, the RNFs from the horizontal raphe are exposed beyond the vertical midline, and the whole foveal tissue is displaced. **D.** Summation (s) of all the vectors of RNF contraction (r) and gravity (g) displace the fovea to the optic disk and slightly downward.

advocate that deformation of the retinal vasculature would be indirect information for the array changes in the photoreceptors. The photoreceptor disarrangement theory is also supported by the current observations that postoperative metamorphopsia directly correlates with macular deformation assessed in the retinal vessels using the square grid: the vertical M-score to the deformation of the vertical line on the fovea and the horizontal M-score to that of the horizontal line.

Interpretation based on the disarrangement theory can explain the results of the previous and current studies, as presented schematically in Figure 6. When an MH develops while elevating the cuff, the patient has pincushion distortion due to the barrel-shape arrangement of the photoreceptors displaced centrifugally (Figure 6A), as claimed by Saito et al.[20] An ideal MH closure results in the recovery of the photoreceptor arrangement and resolution of metamorphopsia (Figure 6B). In the eyes of a small-extent ILM peel, the nasal parafoveal tissues will be deformed because of contraction of the RNFs causing asymmetric elongation of the fovea. Consequently, reduction in metamorphopsia will be less in this group (Figure 6C), which corresponds to the results of the prospective study by Bae et al.[14] If ILM is removed to a large extent, the fovea will be displaced to the optic disk while maintaining the rectangular configuration of the square grid, and perifoveal deformation will be more prominent than the parafoveal deformation, as shown in this study. Accordingly, preoperative pincushion metamorphopsia improved, but postoperative metamorphopsia resulted from the perifoveal deformation (Figure 6D).

There are limitations to this study. First, this was a retrospective study with a small number of eyes and no comparative group. Prospective studies with a larger number of patients are needed to examine the exact mechanism of postoperative metamorphopsia. Second, the preoperative M-score was not measured, and the change was not evaluated. However, as aforementioned, preoperative pincushion distortion is not associated with macular deformation after ILM removal, and our main concerns were to elucidate the association between macular deformation and postoperative metamorphopsia. Finally, the follow-up

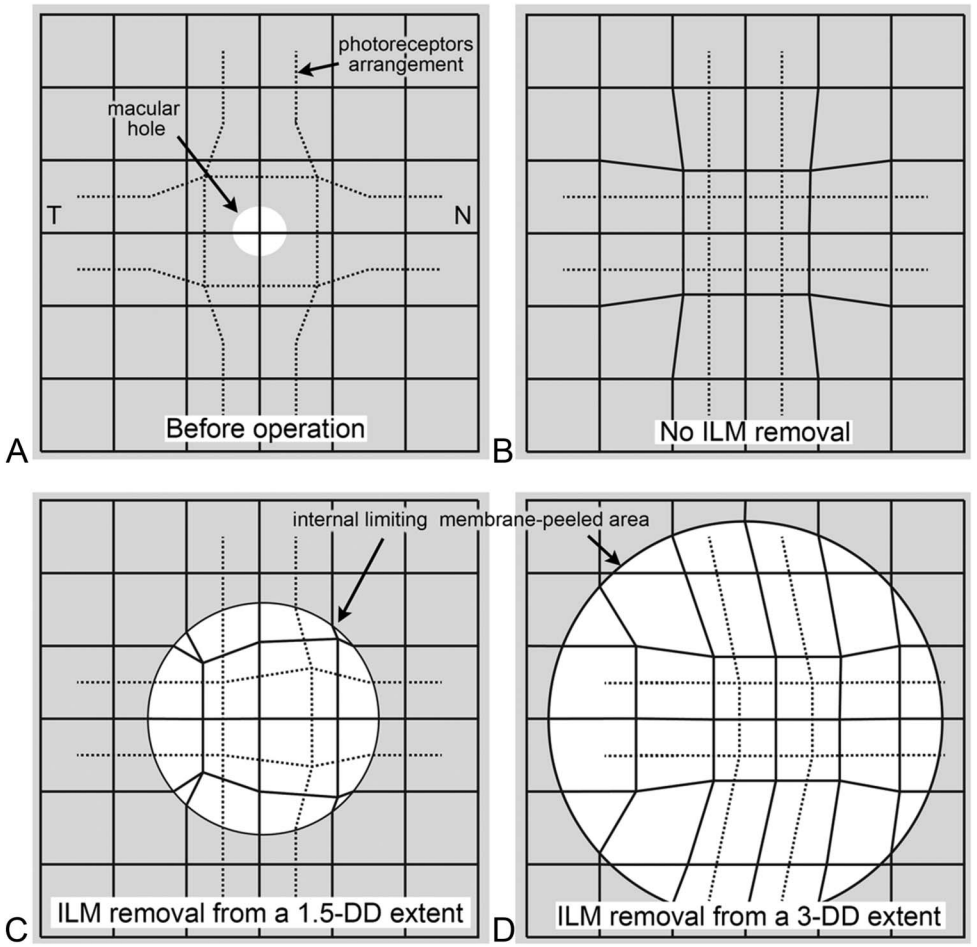

Fig. 6. Schematic drawings to explain the photoreceptor disarrangement theory for metamorphopsia. The dotted lines indicate the arrangement of the photoreceptors. The square grid represents the grid analysis of this study. **A.** The pincushion distortion will result from the barrel-shape arrangement of the photoreceptors displaced centrifugally in the MH. **B.** The photoreceptors returned to the original arrangement with resolution of metamorphopsia after MH closure. **C.** When the ILM is removed to a small extent, the nasal parafoveal tissue is deformed because of the contraction of the RNFs, causing asymmetric elongation of the fovea and less reduction of preoperative metamorphopsia. **D.** A large-extent ILM removal displaces the fovea to the optic disk while maintaining the rectangular configuration of the square grid, and perifoveal deformation is more prominent causing metamorphopsia due to photoreceptor disarrangement.

period might be short to evaluate postoperative deformation of the macula, but it was reported that most of the macular changes related to ILM removal occurs during the first 3 months after operation.[10,16]

In conclusion, the square grid analysis of macular deformation demonstrated that the parafoveal tissue was displaced while retaining the rectangular configuration, causing more prominent perifoveal deformation after ILM removal in MH surgery. The deformed pattern suggested that the postoperative macular deformation depends on the arrangement of the RNFs within the area from where the ILM has been removed. Postoperative horizontal and vertical metamorphopsia correlated not with parafoveal but with perifoveal deformation of the horizontal and vertical lines, respectively. These results propose that photoreceptor disarrangement is the key mechanism for postoperative metamorphopsia.

Key words: foveal deformation, macular hole, M-charts, metamorphopsia, photoreceptor disarrangement.

References

1. Lois N, Burr J, Norrie J, et al; Full-thickness Macular Hole and Internal Limiting Membrane Peeling Study (FILMS) Group. Internal limiting membrane peeling versus no peeling for idiopathic full-thickness macular hole: a pragmatic randomized controlled trial. Invest Ophthalmol Vis Sci 2011;52:1586–1592.
2. Park DW, Sipperley JO, Sneed SR, et al. Macular hole surgery with internal-limiting membrane peeling and intravitreous air. Ophthalmology 1999;106:1392–1397.
3. Park JH, Lee SM, Park SW, et al. Comparative analysis of large macular hole surgery using an internal limiting membrane insertion versus inverted flap technique. Br J Ophthalmol 2019;103:245–250.
4. Michalewska Z, Michalewski J, Adelman RA, Nawrocki J. Inverted internal limiting membrane flap technique for large macular holes. Ophthalmology 2010;117:2018–2025.
5. Nakazawa M, Terasaki H, Yamashita T, et al. Changes in visual field defects during 10-year follow-up for indocyanine green-assisted macular hole surgery. Jpn J Ophthalmol 2016; 60:383–387.
6. Okamoto F, Okamoto Y, Fukuda S, et al. Vision-related quality of life and visual function after vitrectomy for various vitreoretinal disorders. Invest Ophthalmol Vis Sci 2010;51:744–751.

7. Fukuda S, Okamoto F, Yuasa M, et al. Vision-related quality of life and visual function in patients undergoing vitrectomy, gas tamponade and cataract surgery for macular hole. Br J Ophthalmol 2009;93:1595–1599.
8. Yoshikawa M, Murakami T, Nishijima K, et al. Macular migration toward the optic disc after inner limiting membrane peeling for diabetic macular edema. Invest Ophthalmol Vis Sci 2013;54:629–635.
9. Kawano K, Ito Y, Kondo M, et al. Displacement of foveal area toward optic disc after macular hole surgery with internal limiting membrane peeling. Eye (Lond) 2013;27:871–877.
10. Ishida M, Ichikawa Y, Higashida R, et al. Retinal displacement toward optic disc after internal limiting membrane peeling for idiopathic macular hole. Am J Ophthalmol 2014;157:971–977.
11. Pak KY, Park KH, Kim KH, et al. Topographic changes of the macula after closure of idiopathic macular hole. Retina 2017; 37:667–672.
12. Akahori T, Iwase T, Yamamoto K, et al. Macular displacement after vitrectomy in eyes with idiopathic macular hole determined by optical coherence tomography angiography. Am J Ophthalmol 2018;189:111–121.
13. Kim JH, Kang SW, Park DY, et al. Asymmetric elongation of foveal tissue after macular hole surgery and its impact on metamorphopsia. Ophthalmology 2012;119:2133–2140.
14. Bae K, Kang SW, Kim JH, et al. Extent of internal limiting membrane peeling and its impact on macular hole surgery outcomes: a randomized trial. Am J Ophthalmol 2016;169: 179–188.
15. Matsumoto C, Arimura E, Okuyama S, et al. Quantification of metamorphopsia in patients with epiretinal membranes. Invest Ophthalmol Vis Sci 2003;44:4012–4016.
16. Lee SM, Park KH, Kwon HJ, et al. Displacement of the foveal retinal layers after macular hole surgery assessed using en face optical coherence tomography images. Ophthalmic Surg Lasers Imaging Retina 2019;50:414–422.
17. The AREDS Research Group. Change in area of geographic atrophy in the Age-Related Eye Disease Study: AREDS report number 26. Arch Ophthalmol 2009;127:1168–1174.
18. Drasdo N, Fowler CW. Non-linear projection of the retinal image in a wide-angle schematic eye. Br J Ophthalmol 1974; 58:709–714.
19. Ichikawa Y, Imamura Y, Ishida M. Metamorphopsia and tangential retinal displacement after epiretinal membrane surgery. Retina 2017;37:673–679.
20. Saito Y, Hirata Y, Hayashi A, et al. The visual performance and metamorphopsia of patients with macular holes. Arch Ophthalmol 2000;118:41–46.
21. Wollensak G, Spoerl E. Biomechanical characteristics of retina. Retina 2004;24:967–970.
22. Wollensak G, Spoerl E, Grosse G, Wirbelauer C. Biomechanical significance of the human internal limiting lamina. Retina 2006;26:965–968.
23. Conde C, Cáceres A. Microtubule assembly, organization and dynamics in axons and dendrites. Nat Rev Neurosci 2009;10: 319–332.
24. Franze K, Grosche J, Skatchkov SN, et al. Müller cells are living optical fibers in the vertebrate retina. Proc Natl Acad Sci U S A 2007;104:8287–8292.
25. Ichikawa Y, Imamura Y, Ishida M. Inner nuclear layer thickness, a biomarker of metamorphopsia in epiretinal membrane, correlates with tangential retinal displacement. Am J Ophthalmol 2018;193:20–27.
26. Hibi N, Ueno S, Ito Y, et al. Relationship between retinal layer thickness and focal macular electroretinogram components after epiretinal membrane surgery. Invest Ophthalmol Vis Sci 2013;54:7207–7214.